

QCD Predictions for Opposite-Sign Dimuon Production Rates in a Charged-Current Inclusive Neutrino Scattering at High Energies

G. C. Chukwumah

Department of Mathematics, University of Nigeria, Nsukka, Nigeria

Received January 21, 1980

We present our calculations on the predictions of scaling violation for opposite-sign dimuon production rates in a charged-current inclusive neutrino (antineutrino) interaction at high energies, using the QCD-improved parton distribution functions parametrized by Buras and Gaemers, which are in good agreement with various experimental data.

1. INTRODUCTION

Recent high-energy experiments at Fermilab with both muons (Anderson et al., 1976; Watanabe et al., 1975; Chang et al., 1975) and electron beams indicate departures from the predictions based on exact Bjorken scaling. There have also been various experiments to test exact Bjorken scaling in neutrino physics, covering the energy range between 20 and 200 Gev (Berge et al., 1977; Bosetti et al., 1977; Holder et al., 1977; Barish et al., 1977). These experiments suggest departures of about 10%–20% from Bjorken scaling, a level similar to that observed in the muon and electron experiments.

The three main experiments involved were those of the CERN-Dortmund Heidelberg-Saclay (CDHS), the Big European Bubble Chamber (BEBC), and the Caltech Fermilab.

Scale breaking implies that structure functions of the partons depend on the square of the transformed four-momentum Q^2 , as well as x , the fraction of the nucleon four-momentum carried by a parton at low Q^2 .

A number of authors have considered scale-breaking quark models based on asymptotically free theory (ASFT) (Roy et al., 1978; Constantogouris, Gaskell, and Nicolaidis, 1978; Nicolaidis, 1978) and other phenomenological models (Perkins et al., 1977; Frampton and Sakurai, 1977).

These models have already been fitted to the electron and muon data; some of them have also been fitted to the current neutrino and antineutrino charged-current reactions and a satisfactory description of the behavior of quantities most sensitive to scaling violations as a function of energy, has been obtained.

In this paper, we work out predictions of scaling violations for opposite-sign dimuon production rates in charged-current inclusive neutrino and antineutrino interactions at high energies, using the QCD-improved parton distribution functions parametrized by Buras and Gaemers (Buras and Gaemers, 1977a, b, 1978) which are in agreement with various experimental data.

Since it is clear that opposite-sign dimuon events are produced from charmed particles in a charged current interaction, we can conveniently work in the GIM scheme (Glashow, Iliopoulos, and Miani, 1970). The multiplets are given by

$$\begin{pmatrix} e \\ e^- \end{pmatrix}_L, \quad \begin{pmatrix} \mu \\ \mu^- \end{pmatrix}_L, \quad e_R, \quad \mu_R \quad (1.1)$$

$$\begin{pmatrix} u \\ d_\theta \end{pmatrix}_L, \quad \begin{pmatrix} c \\ s_\theta \end{pmatrix}_L, \quad u_R, \quad d_R, \quad s_R, \quad c_R \quad (1.2)$$

where d_θ , s_θ are the Cabibbo rotated quarks, and the rest of the symbols have their usual meanings.

The paper is organized as follows: In Section 2, we present a model of scaling violations based on the QCD-improved parton distribution functions parametrized by Buras et al. (Buras and Gaemers, 1977, 1978). In Section 3, we give numerical estimates of the opposite-sign dimuon production rates as predicted by the model. In Section 4, we compare our results with the recent CDHS, BEBC, and Caltech–Fermilab data, on the one hand, and with the HPWF data, on the other. Finally, we summarize our results and make general comments.

2. A MODEL OF SCALING VIOLATION USING QCD-IMPROVED PARTON DISTRIBUTION FUNCTIONS PARAMETRIZED BY BURAS AND GAEMERS

The approximations of Buras and Gaemers (1977, 1978) for the sea and valence parton distribution functions are given by

$$x\xi(x, Q^2) = \xi_1(Q^2) \left[\frac{\xi_1(Q^2)}{\xi_2(Q^2)} - 1 \right] (1-x)^{\left[\frac{\xi_1(Q^2)}{\xi_2(Q^2)} - 2 \right]} \quad (2.1)$$

$$x\xi^c(x, Q^2) = \xi_1^c(Q^2) \left[\frac{\xi_1^c(Q^2)}{\xi_2^c(Q^2)} - 1 \right] (1-x)^{\left[\frac{\xi_1^c(Q^2)}{\xi_2^c(Q^2)} - 2 \right]} \quad (2.2)$$

and

$$xv(x, Q^2) = \frac{1.5x^{0.7-0.17\ln L}(1-x)^{2.6+0.8\ln L}}{B(0.7-0.176\ln L, 3.6+0.8\ln L)} \quad (2.3)$$

where the beta function is to ensure the zeroth moment sum rule. In equations (2.1), (2.2), and (2.3), the Q^2 -dependent moments of the quark distribution functions are given as follows.

2.1. First Moments.

$$v_1(Q^2) = v_1 L^{-32/75} \quad (2.4)$$

$$\xi_1(Q^2) = \frac{1}{4} \left[\frac{3}{14} + (3\xi_1 + v_1 + \xi_1^c - \frac{3}{14}) L^{-56/75} + (\xi_1 - \xi_1^c - v_1) L^{-32/75} \right] \quad (2.5)$$

$$\xi_1^c(Q^2) = \frac{1}{4} \left[\frac{3}{14} + (3\xi_1 + v_1 + \xi_1^c - \frac{3}{14}) L^{-56/75} - (3\xi_1 - 3\xi_1^c + v_1) L^{-32/75} \right] \quad (2.6)$$

where the moments on the right-hand side are evaluated at a moderately low $Q^2 = Q_0^2$, and

$$L = \ln(Q^2/\Lambda^2)/\ln(Q_0^2/\Lambda^2) \quad (2.7)$$

Λ being the scale-breaking parameter which gives the momentum at which effective gluon coupling constant

$$\alpha_s(Q^2) = \frac{12\pi}{(33-2m)\ln Q^2/\Lambda^2} \quad (2.8)$$

becomes large, m being the number of flavors. The values $0.2 \leq \Lambda \leq 0.5$ ensure that $\alpha_s(Q^2)$ is small enough for $Q^2 \geq 2$ GeV and large for $Q^2 \sim 0.3$ GeV, so that perturbative calculations make sense (De Rujula et al., 1977). The quantity Q_0 is a reference momentum at whose value the scaling quark distribution functions are extracted by fitting low-energy neutrino data.

2.2 Second Moments.

These are given by

$$v_2(Q^2) = v_2 L^{-2/3} \quad (2.9)$$

$$\xi_2(Q^2) = \frac{1}{4} [O_1^2(Q^2) + (\xi_2 - \xi_2^c - v_2) L^{-2/3}] \quad (2.10)$$

$$\xi_2^c(Q^2) = \frac{1}{4} [O_1^2(Q^2) - (3\xi_2 - 3\xi_2^c - v_2) L^{-2/3}] \quad (2.11)$$

where the singlet operator is

$$\begin{aligned} O_1^2(Q^2) = & [0.925(3\xi_2 + \xi_2^c + v_2) + 0.144G_2]L^{-0.609} \\ & + [0.075(3\xi_2 + \xi_2^c - v_2) - 0.144G_2]L^{-1.386} \end{aligned} \quad (2.12)$$

G_2 being the second gluon moment, $v = \frac{1}{2}(v_u + v_d)$ the charge-averaged valence contribution, ξ the $SU(3)$ symmetric sea, and ξ_c the charm component in the sea.

In our calculations we shall use $\Lambda = 0.5$ and $G_2 = 0.057$ (the quantities Λ and G_2 being the only parameters in the model). The value of $\Lambda = 0.5$ is the maximal value of the scale-breaking parameter allowed by the electron and muon data.

We calculate the input moments from the Barger and Phillips parametrization of quark density functions (Barger and Phillips, 1974) given by

$$v_u(x) = 0.594x^{-1/2}(1-x^2)^3 + 0.461x^{-1/2}(1-x^2)^5 + 0.621x^{-1/2}(1-x^2)^7 \quad (2.13)$$

$$v_d(x) = 0.072x^{-1/2}(1-x^2)^3 + 0.206x^{-1/2}(1-x^2)^5 + 0.621x^{-1/2}(1-x^2)^7 \quad (2.14)$$

$$\xi(x) = 0.145x^{-1}(1-x)^9 \quad (2.15)$$

The above parametrization was obtained from fits to SLAC data (Bodek et al., 1973) on $vW_2^{ep,n}F_2^{ep,n}$. In the above, also

$$\begin{aligned} u(x) &= v_u(x) + \xi(x) \\ d(x) &= v_d(x) + \xi(x) \\ \bar{u}(x) &= \bar{d}(x) = s(x) = \bar{s}(x) = \xi(x) \\ v &= \frac{1}{2}(v_u + v_d) \end{aligned} \quad (2.16)$$

Our input moments give

$$\begin{aligned} \xi_1 &\simeq 0.015, & \xi_2 &\simeq 0.0015, & v_1 &\simeq 0.213 \\ \xi_2 &\simeq 0.098 & \text{with } \xi^c &\simeq 0.014 \end{aligned} \quad (2.17)$$

The Q^2 -dependent moments give

$$\xi_1(Q^2) \approx 0.0535 + 0.018 \left(\ln \frac{Q^2}{0.25} \right)^{-0.7467} - 0.066 \left(\ln \frac{Q^2}{0.25} \right)^{-0.4267} \quad (2.18)$$

$$v_1(Q^2) \approx 0.284 \left(\ln \frac{Q^2}{0.25} \right)^{-0.4267} \quad (2.19)$$

$$\xi_1^c(Q^2) \approx 0.0535 + 0.018 \left(\ln \frac{Q^2}{0.25} \right)^{-0.7467} - 0.08 \left(\ln \frac{Q^2}{0.25} \right)^{-0.4267} \quad (2.20)$$

while the Q^2 -dependent quark distributions give

$$x\xi(x, Q^2) \approx \left[0.0535 + 0.018 \left(\ln \frac{Q^2}{0.25} \right)^{-0.7467} - 0.066 \left(\ln \frac{Q^2}{0.25} \right)^{-0.4267} \right] \\ \times \left\{ \frac{0.0535 + 0.018 [\ln(Q^2/0.25)]^{-0.7467} - 0.066 [\ln(Q^2/0.25)]^{-0.4267}}{0.039 [\ln(Q^2/0.25)]^{-0.609} + 0.055 [\ln(Q^2/0.25)]^{-1.386} - 0.038 [\ln(Q^2/0.25)]^{-0.67}} - 1 \right\} (1-x)^{P_1}$$

where

$$P_1 = \left\{ \frac{0.0535 + 0.018 [\ln(Q^2/0.25)]^{-0.7467} - 0.066 [\ln(Q^2/0.25)]^{-0.4267}}{0.039 [\ln(Q^2/0.25)]^{-0.609} + 0.055 [\ln(Q^2/0.25)]^{-1.386} - 0.038 [\ln(Q^2/0.25)]^{-0.67}} - 2 \right\} \quad (2.21)$$

$$x\xi^c(x, Q^2) \approx \left\{ 0.0535 + 0.018 [\ln(Q^2/0.25)]^{-0.7467} - 0.08 [\ln(Q^2/0.25)]^{-0.4267} \right\}$$

$$\times \left\{ \frac{0.0535 + 0.018 [\ln(Q^2/0.25)]^{-0.7467} - 0.08 [\ln(Q^2/0.25)]^{-0.4267}}{0.039 [\ln(Q^2/0.25)]^{-0.609} + 0.055 [\ln(Q^2/0.25)]^{-1.386} - 0.08 [\ln(Q^2/0.25)]^{-0.67}} - 1 \right\} (1-x)^{P_2} \quad (2.22)$$

TABLE I. Summary of Q^2 -Dependent Quark Distribution Functions for Various Values of Q^2

Value of Q^2 (GeV)	Distribution function
4	$x\xi(x, Q^2) \approx 0.005(1-x)^{-0.72}$
	$xv(x, Q^2) \approx \frac{1.5x^{0.45}(1-x)^{3.74}}{B(0.45, 4.74)}$
15	$x\xi(x, Q^2) \approx 0.037(1-x)^{0.56}$
	$xv(x, Q^2) \approx \frac{1.5x^{0.33}(1-x)^{4.28}}{B(0.33, 5.28)}$
20	$x\xi(x, Q^2) \approx 0.04(1-x)^{0.78}$
	$xv(x, Q^2) \approx \frac{1.5x^{0.31}(1-x)^{4.4}}{B(0.31, 5.4)}$

where

$$P_2 = \left\{ \frac{0.0535 + 0.018[\ln(Q^2/0.25)]^{-0.7467} - 0.08[\ln(Q^2/0.25)]^{-0.4267}}{0.039[\ln(Q^2/0.25)]^{-0.609} + 0.055[\ln(Q^2/0.25)]^{-1.386} - 0.04[\ln(Q^2/0.25)]^{-0.67}} - 2 \right\} \quad (2.23)$$

$$xv(x, Q^2) \approx \frac{1.5x^{0.7-0.09\ln(Q^2/0.25)}(1-x)^{2.6+0.41\ln(Q^2/0.25)}}{B[0.7-0.09\ln(Q^2/0.25), 3.6+0.41\ln(Q^2/0.25)]} \quad (2.24)$$

For a summary of Q^2 -dependent quark distribution functions, see Table I.

3. NUMERICAL ESTIMATES FOR THE ν -INDUCED OPPOSITE-SIGN DIMUON PRODUCTION RATES IN THE QCD-IMPROVED QUARK DISTRIBUTION FUNCTIONS

We calculate the following ratios:

$$\sigma^{\nu N}(\mu^- \mu^+)/\sigma^{\nu N}(\mu^-), \quad \sigma^{\bar{\nu} N}(\mu^+ \mu^-)/\sigma^{\bar{\nu} N}(\mu^+),$$

$$\sigma^{\bar{\nu} N}(\mu^+ \mu^-)/\sigma^{\nu N}(\mu^- \mu^+)$$

in the energy region 50–200 GeV, and for values of Q^2 between 4 and 20 GeV, in the GIM scheme. The framework for the various quantities entering the ratios is provided as follows.

3.1. The charged-current neutrino (antineutrino) single-muon cross sections in the scaling quark-parton model are given, in $G^2 ME/\pi$, by (Ndili and Chukwumah, 1977).

(a) *Below Charm Threshold.*

$$\begin{aligned} \frac{d\sigma^{\nu N}}{dx dy}(\mu^-) &= x \left\{ (u(x) + d(x)) \cos^2 \theta_c \right. \\ &\quad \left. + \alpha \cdot [(u(x) + \bar{d}(x))(1-y)^2 + 2s(x) \sin^2 \theta_c] \right\} \quad (3.1) \\ &= x \left\{ (2v(x) + 2\xi(x) \cdot \alpha) \cos^2 \theta_c + \alpha \cdot [2\xi(x)(1-y)^2 + 2\xi(x) \sin^2 \theta_c] \right\} \\ &\quad (3.2) \end{aligned}$$

and

$$\begin{aligned} \frac{d\sigma^{\bar{\nu} N}}{dx dy}(\mu^+) &= x \left\{ (u(x) + d(x))(1-y)^2 \right. \\ &\quad \left. + \alpha \cdot [(\bar{u}(x) + \bar{d}(x)) \cos^2 \theta_c + 2s(x) \sin^2 \theta_c] \right\} \\ &= x \left\{ 2v(x) + 2\xi(x) \alpha(1-y)^2 + \alpha \cdot [2\xi(x) \cos^2 \theta_c + 2\xi(x) \sin^2 \theta_c] \right\} \\ &\quad (3.3) \end{aligned}$$

where α is free parameter measuring the percentage contribution of the sea to valance quarks, with $0 \leq \alpha < 1$, and u, d, s are the up-, down-, and strange quark distribution functions, respectively, while $\bar{u}, \bar{d}, \bar{s}$ are their antiquark distribution functions.

(b) *Above Charm Threshold.* The charmed quark is excited at threshold energy E_{th} , so that the single muon differential cross sections modify, through slow rescaling, to the following:

$$\begin{aligned} \frac{d\sigma^{\nu N}}{dx dy}(\mu^-) &= x \left\{ (u(x) + d(x)) \cos^2 \theta_c \right. \\ &\quad \left. + \alpha \cdot [(\bar{u}(x) + \bar{d}(x))(1-y)^2 + 2s(x) \sin^2 \theta_c] \right\} \\ &\quad + \xi_c (u(\xi_c) + d(\xi_c)) \sin^2 \theta_c Y_c^+ (1 - B_\nu^c) \cdot \\ &\quad + \alpha \cdot (2\xi_c \xi(\xi_c) \cos^2 \theta_c) Y_c^+ (1 - B_\nu^c) \\ &= x \left[2v(x) \cos^2 \theta_c + \alpha \cdot 2\xi(x)(1-y)^2 \right] \\ &\quad + \xi_c \left[2v(\xi_c) \sin^2 \theta_c + \alpha \cdot 2\xi(\xi_c) \right] (1 - B_\nu^c) Y_c^+ \quad (3.4) \end{aligned}$$

$$\begin{aligned}
\frac{d\sigma^{\bar{N}}}{dx dy} &= x \left\{ (u(x) + d(x))(1-y)^2 + \alpha \cdot \left[(\bar{u}(x) + \bar{d}(x)) \cos^2 \theta_c + 2\bar{s}(x) \sin^2 \theta_c \right] \right\} \\
&\quad + \alpha \cdot \left\{ \xi_c (\bar{u}(\xi_c) + \bar{d}(\xi_c)) \sin^2 \theta_c Y_c^+ (1 - B_\nu^c) \right. \\
&\quad \left. + 2\bar{s}(\xi_c) \xi_c Y_c^+ \cos^2 \theta_c (1 - B_\nu^c) \right\} \\
&= x [2v(x)(1-y)^2 + \alpha \cdot \xi(x) (1 + (1-y)^2)] + \alpha \xi_c \cdot 2\xi(\xi_c) Y_c^+ (1 - B_\nu^c)
\end{aligned} \tag{3.5}$$

where slow rescaling is defined by

$$\xi_c = x + \frac{m_c^2}{2MEy} \tag{3.6}$$

m_c being the mass of the charmed quark, M the nucleon mass, and Y_c^+ is given by

$$Y_c^+ = 1 - \frac{m_c^2}{2ME\xi_c} \tag{3.7}$$

3.2. Opposite-Sign Dimuon Cross Sections. In units of $G^2 ME/\pi$, these are given (Ndili and Chukwumah, 1977) by

$$\begin{aligned}
\frac{d\sigma^{\nu N}}{dx dy} (\mu^- \mu^+) &= \xi_c [u(\xi_c) + d(\xi_c)] \sin^2 \theta_c Y_c^+ B_\nu^c \\
&\quad + \alpha \cdot 2\xi_c s(\xi_c) \cos^2 \theta_c Y_c^+ B_\nu^c
\end{aligned} \tag{3.8}$$

$$\begin{aligned}
\frac{d\sigma^{\bar{\nu} N}}{dx dy} (\mu^+ \mu^-) &= \alpha \cdot \xi_c [\bar{u}(\xi_c) + \bar{d}(\xi_c)] \sin^2 \theta_c B_\nu^c Y_c^+ B_{\bar{\nu}}^c \\
&\quad + \alpha \cdot \xi_c \cdot 2s(\xi_c) Y_c^+ \cos^2 \theta_c B_{\bar{\nu}}^c
\end{aligned} \tag{3.9}$$

or alternatively, by

$$\frac{d\sigma^{\nu N}}{dx dy} (\mu^- \mu^+) = \xi_c [2v(\xi_c) \sin^2 \theta_c + \alpha \cdot 2\xi(\xi_c)] B_\nu^c Y_c^+ \tag{3.10}$$

$$\frac{d\sigma^{\bar{\nu} N}}{dx dy} (\mu^+ \mu^-) = \alpha \cdot \xi_c 2\xi(\xi_c) Y_c^+ B_{\bar{\nu}}^c \tag{3.11}$$

In the QCD-improved quark distribution functions parametrized by Buras et al., we have

$$\begin{aligned} \frac{d\sigma^{\nu N}}{dx dy}(\mu^-) = & x \{ 2v(x, Q^2) \cos^2 \theta_c + \alpha \cdot [1 + (1-y)^2] 2\xi(x, Q^2) \} \\ & + \xi_c [2v(\xi_c, Q^2) \sin^2 \theta_c + \alpha \cdot 2\xi(\xi_c, Q^2)] (1 - B_\nu^c) Y_c^+ \end{aligned} \quad (3.12)$$

$$\begin{aligned} \frac{d\sigma^{\bar{\nu} N}}{dx dy}(\mu^+) = & x \{ 2v(x, Q^2) (1-y)^2 + \alpha \cdot [1 + (1-y)^2] \cdot 2\xi(x, Q^2) \} \\ & + \alpha \xi_c \cdot 2\xi(\xi_c, Q^2) Y_c^+ (1 - B_{\bar{\nu}}^c) \end{aligned} \quad (3.13)$$

$$\frac{d\sigma^{\nu \bar{\nu}}}{dx dy}(\mu^- \mu^+) = \xi_c [2v(\xi_c, Q^2) \sin^2 \theta_c + \alpha \cdot 2\xi(\xi_c, Q^2)] Y_c^+ (1 - B_\nu^c) \quad (3.14)$$

$$\frac{d\sigma^{\bar{\nu} \nu}}{dx dy}(\mu^+ \mu^-) = \alpha \cdot \xi_c \cdot 2\xi(\xi_c, Q^2) Y_c^+ B_{\bar{\nu}}^c \quad (3.15)$$

3.3. Bounds on the Integration Variables x, y, ξ_c, y_c for Total Cross Sections. For $Q_0^2 \ll Q^2$, the bounds on the integration variables for the total cross sections of quantities of interest are given by the following:

(a) For light quarks in the final state $(u, d, s, \bar{u}, \bar{d}, \bar{s})$, we have

$$\frac{Q_0^2}{2ME} \leq x \leq 1, \quad \frac{Q_0^2}{2ME} \leq y \leq 1 \quad (3.16)$$

(b) For charmed quarks in the final state, we have

$$\begin{aligned} \frac{Q_0^2}{2ME} \leq x_c \leq 1 - \frac{m_c^2}{2ME} \\ \frac{m_c^2 + Q_0^2}{2ME} \leq y_c \leq 1 \\ \frac{m_c^2 + Q_0^2}{2ME} \leq \xi_c \leq 1 \end{aligned} \quad (3.17)$$

3.4. Predictions from QCD for the Rates of Dimuon Relative to Single-Muon Production. We integrate the appropriate differential cross sections, using the bounds in Section 3.3, to obtain the following tables of

predictions of the QCD-improved parton distribution functions parametrized by Buras and Gaemers, for the rates of dimuon relative to single muon production, at various incident neutrino (antineutrino) energies (50–200 GeV.) and for values of Q^2 in the range 4–20 GeV.

We take the estimated ratio of antiquark to quark distributions, α , to lie between 0.1 and 0.2.

4. QCD PREDICTIONS FOR $\sigma(\mu^\mp\mu^\pm)/\sigma(\mu^\mp)$ COMPARED WITH EXPERIMENTAL DATA

We have carried out detailed calculations of the predictions of the QCD-improved parton distribution functions parametrized by Buras and Gaemers, for opposite-sign dimuon production ratios: $\sigma(\mu^-\mu^+)/\sigma(\mu^-)$, $\sigma(\mu^+\mu^-)/\sigma(\mu^+)$, and $\sigma(\mu^+\mu^-)/\sigma(\mu^-)$, in a charged-current inclusive neutrino and antineutrino scattering, at high energies.

The results of our computations are given in the form of tables and figures. We have obtained two sets of tables and figures. The first set of tables and figures gives $\sigma^{\nu N}(\mu^-\mu^+)/\sigma^{\nu N}(\mu^-)$, $\sigma^{\bar{\nu} N}(\mu^+\mu^-)/\sigma^{\bar{\nu} N}(\mu^+)$, and $\sigma^{\bar{\nu} N}(\mu^+\mu^-)/\sigma^{\nu N}(\mu^-\mu^+)$, as functions of the incident neutrino and/or antineutrino energies, for fixed Q^2 , the square of the transferred four-momentum. The second set of tables and figures shows the same quantities as functions of Q^2 , for fixed E^s . The tables and figures have been obtained for the following parameters of the theory and estimates of quantities:

$$\Lambda = 0.5, \quad G^2 = 0.057, \quad \alpha = 0.1, 0.15, \text{ and } 0.2 \\ B_\nu^c = B_{\bar{\nu}}^c \approx 0.15 \quad (4.1)$$

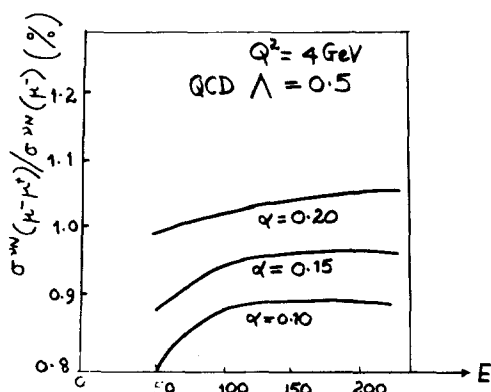


Fig. 1. $\sigma^{\nu N}(\mu^-\mu^+)/\sigma^{\nu N}(\mu^-)$ as a function of E_ν , for fixed Q^2 (= 4 GeV).

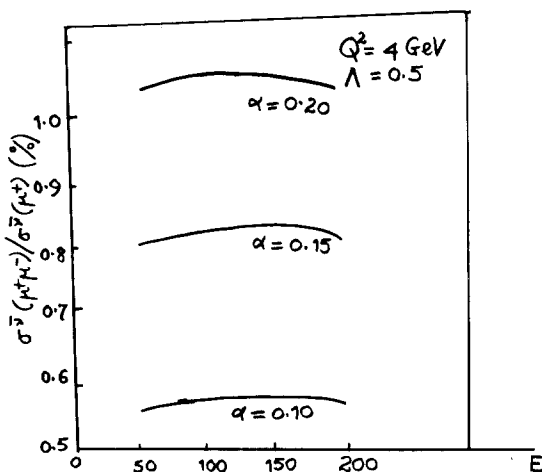


Fig. 2. $\sigma(\bar{\nu}N(\mu^+\mu^-))/\sigma(\bar{\nu}N(\mu^+)$ as a function of $E_{\bar{\nu},\bar{\nu}}$ for fixed $Q^2 (=4 \text{ GeV})$, $\Lambda=0.5$, $B^* \approx 0.15$.

At low $Q^2 (Q^2 \sim 4 \text{ GeV})$ and for $E < 150 \text{ GeV}$, the predicted rates for $\sigma^{\nu N}(\mu^-\mu^+)/\sigma^{\nu N}(\mu^-)$ and $\sigma^{\bar{\nu}N}(\mu^+\mu^-)/\sigma^{\bar{\nu}N}(\mu^+)$ (Figures 1 and 2) are in poor agreement with the recent CDHS and CITFR data (Fox, 1978; see Figure 14). However, the same rates are in reasonably good agreement with the lower limits of the HPWF experimental data (Benvenuti et al., 1975; Rubbia, 1975):

$$\sigma(\mu^-\mu^+)/\sigma(\mu^-) \approx 0.008 \pm 0.003 \quad (4.2)$$

$$\sigma(\mu^+\mu^-)/\sigma(\mu^+) \approx 0.02 \pm 0.01 \quad (4.3)$$

In the region of the very high E and $Q^2 (E > 150 \text{ GeV}, Q^2 \geq 15)$ the scale-violating QCD-model predictions for $\sigma(\mu^\mp\mu^\pm)/\sigma(\mu^\mp)$ (Figures 3–5, 8–13) are in excellent agreement with the CDHS and CITFR data (Fox, 1978; see Fig. 14).

Also in this region, the prediction of the model for $\sigma(\mu^-\mu^+)/\sigma(\mu^-)$ is in excellent agreement with the upper limit of the HPWF data, while the same predictions of the model for $\sigma(\mu^+\mu^-)/\sigma(\mu^+)$ are lower than the upper limits of the HPWF data. It appears then that one of the effects of the Q^2 -dependent quark density function parametrization of Buras and Gaemers on opposite-sign dimuon production rates on a charged-current inclusive neutrino and antineutrino scattering at high energies is to reduce the upper limit of the HPWF rate for $\sigma(\mu^+\mu^-)/\sigma(\mu^+)$.

However, more precise data on $\sigma(\mu^+\mu^-)/\sigma(\mu^+)$ are needed before the above observation can have any import.

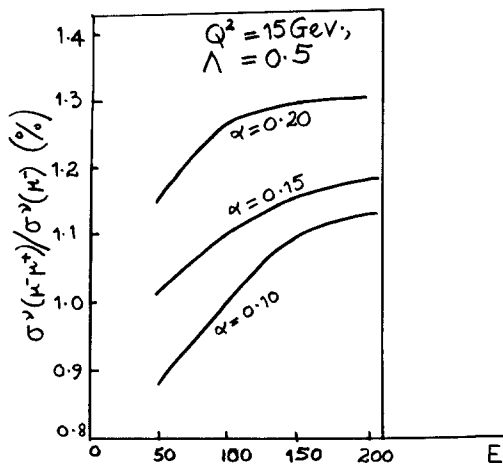


Fig. 3. $\sigma^{\nu N}(\mu^- \mu^+)/\sigma^{\nu N}(\mu^-)$ as a function of E for fixed Q^2 ($= 15 \text{ GeV}$).

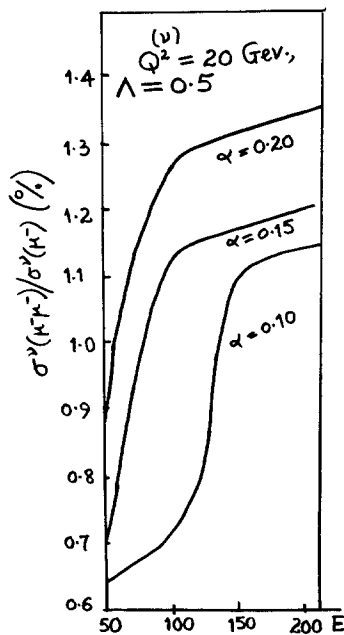


Fig. 4. $\sigma^{\nu N}(\mu^- \mu^+)/\sigma^{\nu N}(\mu^-)$ as a function of E , for fixed Q^2 ($= 20 \text{ GeV}$).

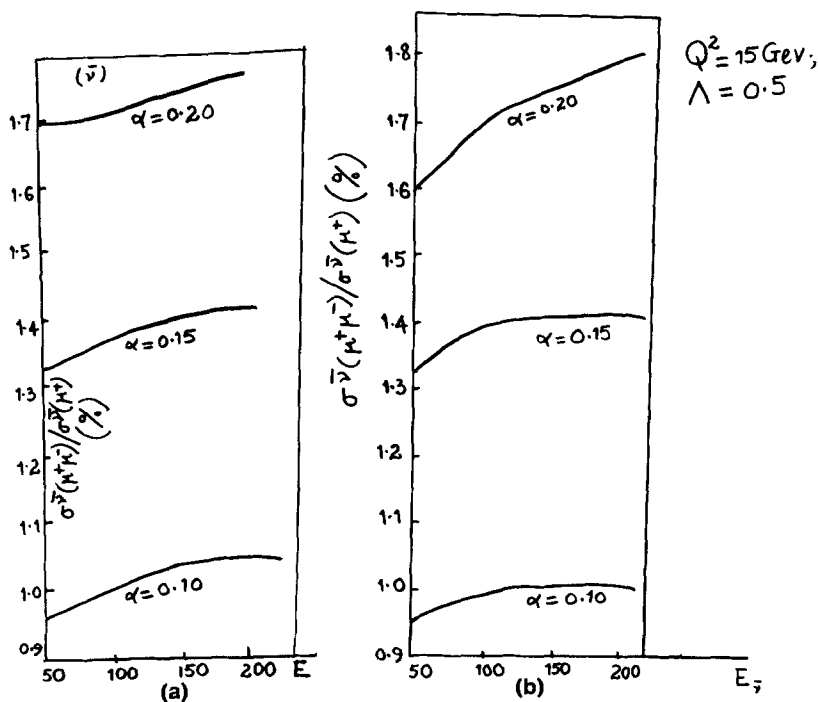


Fig. 5. (a) $\sigma^{\bar{\nu}N}(\mu^+\mu^-)/\sigma^{\bar{\nu}N}(\mu^+)$ as a function of $E_{\bar{\nu}}$, for fixed Q^2 ($=20$ GeV). (b) $\sigma^{\bar{\nu}N}(\mu^+\mu^-)/\sigma^{\bar{\nu}N}(\mu^+)$ as a function of $E_{\bar{\nu}}$ for fixed Q^2 ($=15$ GeV).

TABLE II. Dimuon Ratios vs $E^s_{\nu, \bar{\nu}}$ for Fixed Q^2 ($=4$ GeV)

E (GeV)	Q^2 (GeV)	α	$\frac{\sigma^{\nu N}(\mu^-\mu^+)}{\sigma^{\nu N}(\mu^-)}$	$\frac{\sigma^{\bar{\nu}N}(\mu^+\mu^-)}{\sigma^{\bar{\nu}N}(\mu^+)}$	$\frac{\sigma^{\bar{\nu}N}(\mu^+\mu^-)}{\sigma^{\bar{\nu}N}(\mu^-\mu^+)}$
50	4	0.10	0.0080	0.0056	0.2440
		0.15	0.0087	0.0081	0.320
		0.20	0.0099	0.0104	0.390
100	4	0.10	0.0088	0.0057	0.2330
		0.15	0.0094	0.0083	0.3131
		0.20	0.0102	0.0106	0.3783
150	4	0.10	0.0087	0.0057	0.226
		0.15	0.0096	0.0084	0.3100
		0.20	0.0104	0.0105	0.3800
200	4	0.10	0.0088	0.0057	0.2236
		0.15	0.0096	0.0081	0.3019
		0.20	0.0105	0.0104	0.3700

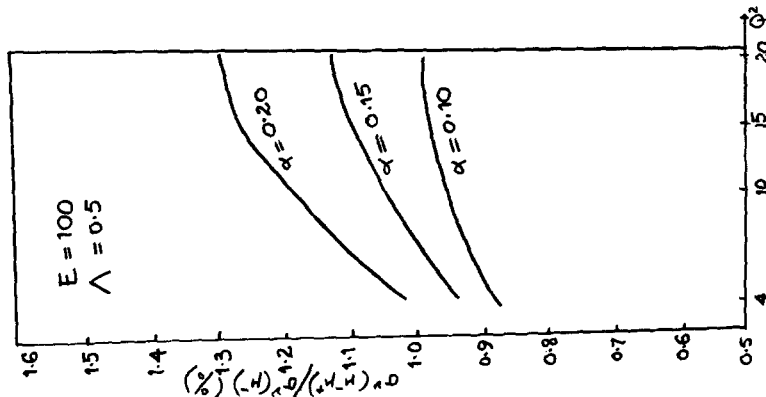


Fig. 6. $\sigma^N(\mu^- \mu^+)/\sigma^N(\mu^-)$ as a function of Q^2 , for fixed $E_p = 50$ GeV.

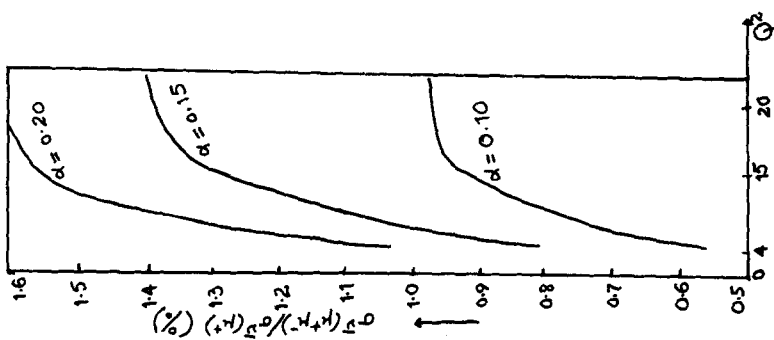


Fig. 7. $\sigma^N(\mu^+ \mu^-)/\sigma^N(\mu^+)$ as a function of Q^2 , for fixed $E_p = 100$ GeV.

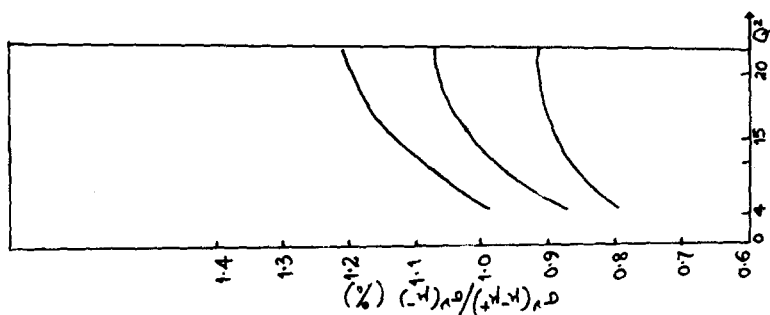


Fig. 8. $\sigma^N(\mu^- \mu^+)/\sigma^N(\mu^-)$ as a function of Q^2 , for fixed $E_p = 100$ GeV.

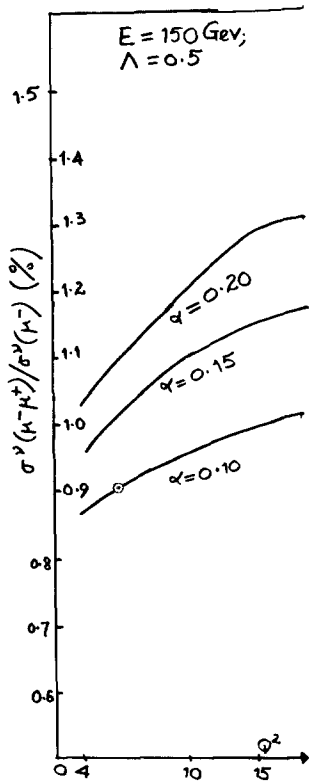


Fig. 9. $\sigma^{\nu N}(\mu^- \mu^+)/\sigma^{\nu N}(\mu^-)$ as a function of Q^2 , for fixed $E_\nu = 150$ GeV.

TABLE III. Dimuon Ratios vs $E_{\nu, \bar{\nu}}$ for Fixed $Q^2 (= 15$ GeV)

$E_{\nu, \bar{\nu}}$ (GeV)	Q^2 (GeV)	α	$\frac{\sigma^{\nu N}(\mu^- \mu^+)}{\sigma^{\nu N}(\mu^-)}$	$\frac{\sigma^{\bar{\nu} N}(\mu^+ \mu^-)}{\sigma^{\bar{\nu} N}(\mu^+)}$	$\frac{\sigma^{\bar{\nu} N}(\mu^+ \mu^-)}{\sigma^{\nu N}(\mu^- \mu^+)}$
50	15	0.10	0.0080	0.0095	0.3870
		0.15	0.0102	0.0132	0.4868
		0.20	0.0116	0.0160	0.5600
100	15	0.10	0.0098	0.0099	0.3620
		0.15	0.0110	0.0139	0.4600
		0.20	0.0127	0.0170	0.05310
150	15	0.10	0.0100	0.0100	0.3619
		0.15	0.0115	0.0139	0.4597
		0.20	0.0129	0.0173	0.5300
200	15	0.10	0.0102	0.0100	0.3560
		0.15	0.0117	0.0140	0.4532
		0.20	0.0130	0.0174	0.5249

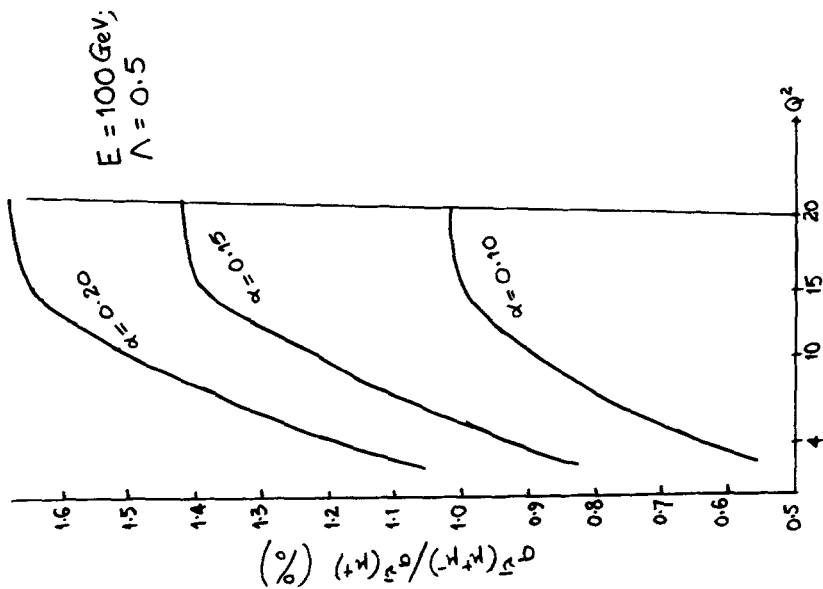


Fig. 11. $\sigma^{\bar{\nu}N}(\mu^+ \mu^-)/\sigma^{\bar{\nu}N}(\mu^+ \mu^+)$ as a function of Q^2 , for fixed $E_\nu = 100 \text{ GeV}$.

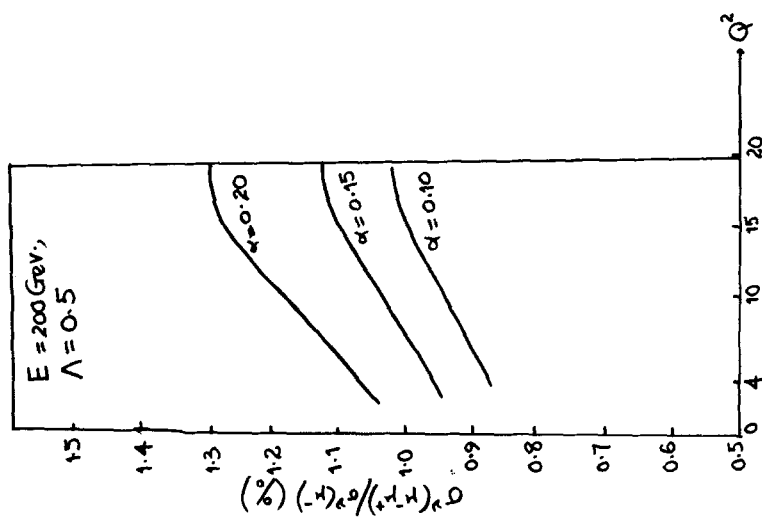


Fig. 10. $\sigma^{\bar{\nu}N}(\mu^- \mu^+)/\sigma^{\bar{\nu}N}(\mu^- \mu^-)$ as a function of Q^2 for fixed incident neutrino energy $E_\nu = 200 \text{ GeV}$.

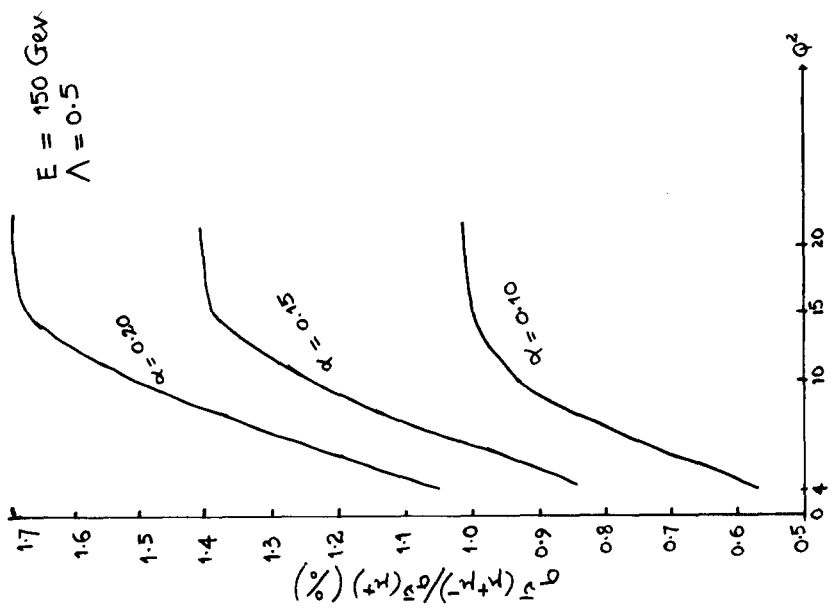


Fig. 12. $\sigma_{\bar{\nu}N}(\mu^+\mu^+)/\sigma_{\bar{\nu}N}(\mu^+)$ as a function of Q^2 , for fixed $E_\nu = 150 \text{ GeV}$.

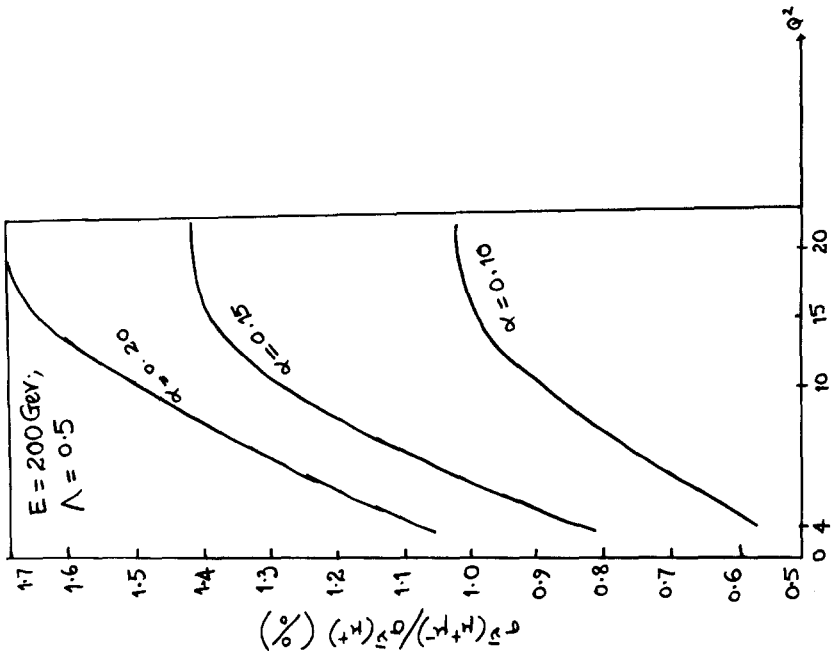


Fig. 13. $\sigma_{\bar{\nu}N}(\mu^+\mu^-)/\sigma_{\bar{\nu}N}(\mu^-)$ vs Q^2 , for fixed $E_\nu = 200 \text{ GeV}$.

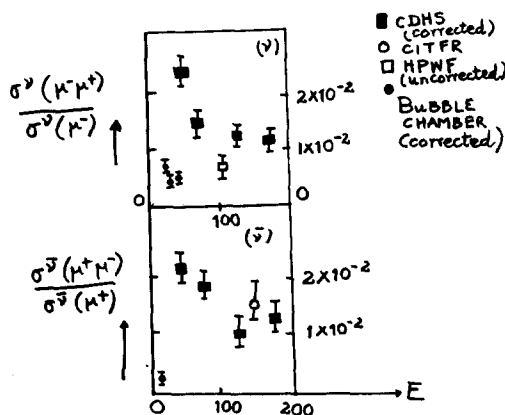


Fig. 14. CDHS, CITFR, HPWF, BEBC data on $\sigma(\mu^+\mu^+)/\sigma(\mu^+)$ at high energies.

Next, we compare the scaling QPM predictions for the neutrino- and antineutrino-induced unequal-sign dimuon production relative to the single muon events, with the scale-violating-QCD predictions for the quantities, at high energies. On the basis of our earlier work on the scaling QPM predictions for $\sigma(\mu^\mp\mu^\pm)/\sigma(\mu^\mp)$ at high energies, in the GIM scheme (Ndili and Chukwumah, 1977), we make this observation: The predictions of both theoretical models for the quantities of interest appear to agree quantitatively, if a rather large proportion of the sea quarks relative to the

TABLE IV. Dimuon Ratios vs $E_{\nu,\bar{\nu}}$ for Fixed $Q^2 (= 20 \text{ GeV})$

$E_{\nu,\bar{\nu}}$ (GeV)	Q^2 (GeV)	α	$\frac{\sigma^{eN}(\mu^- \mu^+)}{\sigma^{eN}(\mu^-)}$	$\frac{\sigma^{\bar{e}N}(\mu^+ \mu^-)}{\sigma^{\bar{e}N}(\mu^+)}$	$\frac{\sigma^{\bar{e}N}(\mu^+ \mu^-)}{\sigma^{eN}(\mu^- \mu^+)}$
50	20	0.10	0.0064	0.0097	0.3826
		0.15	0.0065	0.0139	0.4842
		0.20	0.0066	0.0178	0.5580
100	20	0.10	0.0099	0.0098	0.3635
		0.15	0.0113	0.0137	0.4614
		0.20	0.0127	0.0170	0.5330
150	20	0.10	0.0120	0.0101	0.3661
		0.15	0.0177	0.0140	0.4644
		0.20	0.0130	0.0174	0.5366
200	20	0.10	0.0104	0.0102	0.3621
		0.15	0.0119	0.0142	0.4599
		0.20	0.0134	0.0177	0.5317

TABLE V. Dimuon Ratios vs Q^2 , for a Fixed $E_{\nu,\bar{\nu}}$ ($= 50$ GeV)

$E_{\nu,\bar{\nu}}$ (GeV)	Q^2 (GeV)	α	$\frac{\sigma^{\nu N}(\mu^-\mu^+)}{\sigma^{\nu N}(\mu^-)}$	$\frac{\sigma^{\bar{\nu} N}(\mu^+\mu^-)}{\sigma^{\bar{\nu} N}(\mu^+)}$	$\frac{\sigma^{\bar{\nu} N}(\mu^+\mu^-)}{\sigma^{\nu N}(\mu^-\mu^+)}$
50	4	0.10	0.0080	0.0056	0.2440
		0.15	0.0087	0.0081	0.3200
		0.20	0.0099	0.0104	0.3900
50	15	0.10	0.0088	0.0095	0.3870
		0.15	0.0120	0.0132	0.4868
		0.20	0.0115	0.0160	0.5600
50	20	0.10	0.0090	0.0097	0.3825
		0.15	0.0105	0.0139	0.4842
		0.20	0.1180	0.0178	0.558

valence quarks is allowed to contribute to the cross sections in the former model (scaling QPM), while in the latter model (the scale-violating-QCD model) a low proportion of the sea quarks relative to the valence ones is allowed to contribute to the cross sections. A sea quark contribution as little as 10%–20%, relative to the valence contribution, appears to be experimentally acceptable (Fox, 1978; Perkins, 1975; Barish, 1975).

Finally, the agreement of the predictions of the scale-violating-QCD model of Buras and Gaemers for the unequal-sign dimuon ratios $\sigma(\mu^\mp\mu^\pm)/\sigma(\mu^\mp)$ at high energies, with the recent CDHS and CITFR experimental data in the region of the very high E and Q^2 specified in our analysis, demonstrates, in a way, another success of the model in describing quantities that are sensitive to scaling violations in inclusive neutrino and antineutrino interactions at high energies.

TABLE VI. Dimuon Ratios vs Q^2 , for Fixed $E_{\nu,\bar{\nu}}$ ($= 100$ GeV)

$E_{\nu,\bar{\nu}}$ (GeV)	Q^2 (GeV)	α	$\frac{\sigma^{\nu N}(\mu^-\mu^+)}{\sigma^{\nu N}(\mu^-)}$	$\frac{\sigma^{\bar{\nu} N}(\mu^+\mu^-)}{\sigma^{\bar{\nu} N}(\mu^+)}$	$\frac{\sigma^{\bar{\nu} N}(\mu^+\mu^-)}{\sigma^{\nu N}(\mu^-\mu^+)}$
100	4	0.10	0.0088	0.0057	0.2300
		0.15	0.0094	0.0083	0.3130
		0.20	0.0102	0.0106	0.3800
100	15	0.10	0.0098	0.0099	0.3620
		0.15	0.0110	0.139	0.4600
		0.20	0.0127	0.0170	0.5310
100	20	0.10	0.099	0.0098	0.3635
		0.15	0.0113	0.0137	0.4614
		0.20	0.0127	0.0170	0.5330

TABLE VII. Dimuon Ratios vs Q^2 , for Fixed $E_{\nu, \bar{\nu}}$ (= 150 GeV)

$E_{\nu, \bar{\nu}}$ (GeV)	Q^2 (GeV)	α	$\frac{\sigma^{\nu N}(\mu^- \mu^+)}{\sigma^{\nu N}(\mu^-)}$	$\frac{\sigma^{\bar{\nu} N}(\mu^+ \mu^-)}{\sigma^{\bar{\nu} N}(\mu^+)}$	$\frac{\sigma^{\bar{\nu} N}(\mu^+ \mu^-)}{\sigma^{\nu N}(\mu^- \mu^+)}$
150	4	0.10	0.0087	0.0057	0.2300
		0.15	0.0096	0.0084	0.3100
		0.20	0.0104	0.0105	0.3800
150	15	0.10	0.0100	0.0100	0.3619
		0.15	0.0115	0.0139	0.4597
		0.20	0.0129	0.0173	0.5300
150	20	0.10	0.0120	0.0101	0.3661
		0.15	0.0117	0.0140	0.4644
		0.20	0.0130	0.0174	0.5365

TABLE VIII. Dimuon Ratios vs Q^2 , for Fixed $E_{\nu, \bar{\nu}}$ (= 200 GeV)

$E_{\nu, \bar{\nu}}$ (GeV)	Q^2 (GeV)	α	$\frac{\sigma^{\nu N}(\mu^- \mu^+)}{\sigma^{\nu N}(\mu^-)}$	$\frac{\sigma^{\bar{\nu} N}(\mu^+ \mu^-)}{\sigma^{\bar{\nu} N}(\mu^+)}$	$\frac{\sigma^{\bar{\nu} N}(\mu^+ \mu^-)}{\sigma^{\nu N}(\mu^- \mu^+)}$
200	4	0.10	0.0088	0.0057	0.2238
		0.15	0.0096	0.0081	0.30187
		0.20	0.0105	0.0104	0.3700
200	15	0.10	0.0098	0.0099	0.3619
		0.15	0.0110	0.0139	0.4597
		0.20	0.0127	0.0170	0.5300
200	20	0.10	0.0104	0.0102	0.3621
		0.15	0.0119	0.0142	0.4599
		0.20	0.0134	0.0177	0.5317

REFERENCES

- Anderson, H. L., et al. (1976). *Physical Review Letters*, **37**, 4.
 Anderson, H. L., et al. (1977). *Physical Review Letters*, **38**, 1450.
 Barger, V., and Phillips, R. J. N. (1974). *Nuclear Physics B*, **73**, 269.
 Barish, B. C. (1975). Paper presented at SLAC Conference (1975).
 Barish, B. C., et al. (1977). *Physical Review Letters*, **39**, 741, 1595.
 Benvenuti, A., et al. (1975). *Physical Review Letters*, **35**, 1199, 1203, 1249; **34**, 419.
 Berge, J. P., et al. (1977). *Physical Review Letters*, **39**, 382.
 Bodek, A., et al. (1973). *Physical Review Letters*, **30**, 1087.
 Bosetti, P. C., et al. (1977). *Physics Letters*, **70B**, 273.
 Buras, A. J., and Gaemers, K. J. F. (1977a). CERN Preprint: CERN TH. 2322.
 Buras, A. J., and Gaemers, K. J. F. (1977b). *Physics Letters*, **71B**, 106.
 Buras, A. J., and Gaemers, K. J. F. (1978). *Nuclear Physics*, **B132**, 349.

- Chang, C., et al. (1975). *Physical Review Letters*, **35**, 901.
- Contogouris, A. P., Gaskell, R., and Nicolaïdis, A. (1978). *Physical Review D*, **17**, 2992.
- De Rujula, A., Georgi, H., Politzer, H. D. (1977). *Annals of Physics*, **103**, 315.
- Fox, G. C. (1978). "The Physics of Inclusive Charged Current Neutrino Reactions," CALT-68-658, pp. 22.
- Frampton, P. H., and Sakurai, J. J. (1977). "Model for Scaling Violation," UCLA Preprint UCLA/77/TEP/3.
- Glashow, S. L., Iliopoulos, J., and Maiani, L. (1970). *Physical Review D*, **2**, 1285.
- Holder, M. et al. (1977). *Physical Review Letters*, **39**, 433.
- Ndili, F. N. and Chukwumah, G. C. (1977). *Physical Review D*, **15**, 1227.
- Nicolaïdis, A. (1978). "Scaling Deviations in charged current neutrino reactions," McGill University Preprint.
- Perkins, D. H. (1975). Paper presented at SLAC Conference.
- Perkins, D. H., Schreiner, P. and Scott, W. G. (1977). *Physics Letters*, **67B**, 347.
- Roy, D. P., Paranjape, S., Pardita, P.N., and Choudhury, D. K. (1978). Tata Institute Preprint.
- Rubbia, C. (1975). Paper presented at the Institute of Particle Physics International Summer School, Montreal (unpublished); see also paper presented at the EPS International Conference on High Energy Physics, Palermo (1975) (unpublished).
- Watanabe, Y. et al., (1975). *Physical Review Letters*, **35**, 898.